Available online at www.sciencedirect.com
ScienceDirect
Journal of Organometallic Chemistry 692 (2007) 3223–3230
Journal of Organometallic Chemistry
www.elsevier.com/locate/jorganchem

Oxidatively induced reactions of a diimine platinum(IV) tetramethyl complex

Bror J. Wik, Mats Tilset *

Department of Chemistry, University of Oslo, P.O. Box 1033 Blindern, N-0315 Oslo, Norway

Received 22 December 2006; received in revised form 23 February 2007; accepted 23 February 2007
Available online 12 March 2007

Abstract

The oxidation of the Pt(IV) tetramethyl complex [Ar—N=CH—CH=N—Ar]$PtMe_4$ (Ar = 2,6-$Me_2C_6H_3$) has been investigated in acetonitrile and dichloromethane. Cyclic voltammetry demonstrates that the irreversible oxidation of [Ar—N=CH—CH=N—Ar]$PtMe_4$ occurs at a slightly less positive oxidation potential than the irreversible oxidation of the analogous Pt(II) species [Ar—N=CH—CH=N—Ar]$PtMe_2$. The product distribution arising from the oxidation depends strongly on the reaction conditions and includes cationic Pt(IV) species (acetonitrile, dichloromethane solvents) and Pt(II) species (dichloromethane only). Evidence is presented that suggests that homolytic cleavage of a weakened Pt—C bond in [ArN=CH—CH=NAr]$PtMe_4^{\cdot+}$ is involved in the oxidatively induced reactions.

Keywords: Platinum methyl; Pt(IV); Oxidation; Cyclic voltammetry; Homolysis; Diimine

1. Introduction

More than 35 years ago, Garnett and Hodges [1,2] demonstrated that aromatic C—H bonds could be activated by aqueous Pt(II) salts, and the Shilov group [3–5] discovered shortly thereafter that even the more unreactive aliphatic C—H bonds can be similarly activated and functionalized. Since then, substantial efforts have been made to understand the mechanistic details of such reactions, both on what is commonly termed the "Shilov system" and on organometallic model systems [6–8]. As a result of these efforts, the general mechanism that is depicted in Scheme 1 has emerged for the C—H functionalization by the Shilov system.

We and others have reported that protonation of α-diimine Pt(II) complexes (N—N)$PtMe_2$ (N—N = aryl-N=CR—CR=N-aryl; aryl = substituted phenyl and R = H/Me) in trifluoroethanol generates species that activate aliphatic and aromatic C—H bonds under mild conditions [9–11]. The up-to-date mechanistic insight that pertains to the C—H activation step in Scheme 1 was recently reviewed [6]. Some time ago [12], we investigated the chemical and electrochemical oxidation chemistry of (N—N)$PtMe_2$ complexes, obviously of relevance to the oxidation step in Scheme 1. The primary oxidatively induced reaction in solution was found to be a methyl transfer process, formally a disproportionation of two transient Pt(III) species, to furnish the cationic Pt(II) and Pt(IV) products that are depicted in Scheme 2.

Cyclic voltammograms of (N—N)$PtMe_2$ species reveal well-defined, reversible reduction waves, whereas the oxidation process is irreversible and rather ill-defined [12] with peak potentials around +0.6 V vs. $Cp_2Fe^{0/+}$; thermodynamically significant electrode potentials could not be extracted with the desired accuracy. Bercaw and co-workers [13] investigated the Pt(II)/Pt(IV) oxidation process via outer-sphere oxidations (i.e. equilibrium measurements of anionic ligand exchange reactions). Kaim and co-workers reported a rare case of a reversible one-electron oxidation of a diimine Pt(II) complex, (Cy—N=CH—CH=N—Cy)Pt(mesityl)$_2$ [14]. Interestingly, irreversible electro-

* Corresponding author.
E-mail address: mats.tilset@kjemi.uio.no (M. Tilset).

0022-328X/$ - see front matter © 2007 Elsevier B.V. All rights reserved.
doi:10.1016/j.jorganchem.2007.02.040

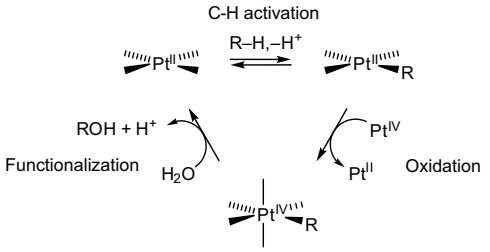

Scheme 1.

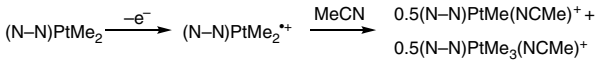

Scheme 2.

chemical oxidation potentials for Pt(II) and Pt(IV) complexes (N—N)$PtMe_2$ and (N—N)$PtMe_4$ were found to be quite similar, and it was concluded [14] that "...the binding of two additional methyl carbanions compensates almost exactly for the effect of the higher metal oxidation state." If Pt(IV) complexes are indeed as readily oxidized as closely related Pt(II) species that are involved in C—H activation reactions, it will obviously be of great relevance to understand the oxidation chemistry of Pt(IV) species in detail in relation to the Shilov chemistry.

In this work, we present some results of an investigation of the oxidation chemistry of a Pt(IV) diimine complex (Ar—N=CH—CH=N—Ar)$PtMe_4$ (**1**) where Ar = 2,6-$Me_2C_6H_3$. It will be demonstrated that a homolytic Pt—*Me* bond cleavage is likely to be a key step in much of the oxidatively induced reactivity of **1**.

2. Experimental part

2.1. General procedures

^{1}H NMR spectra were recorded on Bruker Avance DPX 200 and 300 instruments. ^{1}H NMR shifts are reported in parts per million relative to tetramethylsilane, with the residual solvent peak as internal standard. All handling of organometallic compounds were done under an atmosphere of N_2 with the use of standard Schlenk or drybox techniques. The Pt(IV) complex **1** is particularly photosensitive [14], so all handling of this material was done with minimum exposure to light. Elemental analyses were performed by Ilse Beetz Mikroanalytisches Laboratorium, Kronach, Germany. For electrochemical measurements, acetonitrile and dichloromethane containing the supporting electrolyte were passed through a column of active neutral alumina to remove water and acidic impurities. The electrolyte was freed of air by purging with purified and solvent saturated argon, and all measurements were carried out under a blanket of argon. Electrochemical measurements were performed with an EG&G-PAR Model 273 Potentiostat/Galvanostat. The working electrodes were Pt disc electrodes ($d = 0.6$ mm), the counter electrode was a Pt wire, and the Ag wire reference electrode assembly was filled with acetonitrile/0.01 M $AgNO_3$/0.1 M $Bu_4N^+PF_6^-$. The reference electrode was calibrated against $Cp_2Fe^{0/+}$, which was also used as reference in this work. The positive feedback *iR* compensation circuitry of the potentiostat was employed; the separation of anodic and cathodic peaks for Cp_2Fe oxidation was 60–62 mV in acetonitrile.

The diimine ligand Ar—N=CH—CH=N—Ar [15], $Pt_2Me_8(\mu\text{—}SMe_2)_2$ [16], $Pt_2Me_4(\mu\text{—}SMe_2)_2$ [17], and $Cp_2Fe^+OTf^-$ [18] were prepared by published procedures. All other reagents were purchased from commercial suppliers and used as obtained.

2.2. Synthesis of [Ar—N=CH—CH=N—Ar]$PtMe_4$ [Ar = 2,6-$Me_2C_6H_3$] (**1**)

The diimine ligand (110 mg, 0.42 mmol) was added to a suspension of $Pt_2Me_8(\mu\text{-}SMe_2)_2$ (120 mg, 0.19 mmol) in dry diethyl ether (20 mL) and the mixture was stirred for 17 h. The product was isolated by removal of the solvent, and washed with pentane. Removal of the residual solvents by evaporation produced pure material in 76% yield. ^{1}H NMR (200 MHz, $CDCl_3$) δ −0.05 (s, ^2J(^{195}Pt—H) = 46.0 Hz, 6H, Pt—Me_{ax}), 0.60 (s, ^2J(^{195}Pt—H) = 72.8 Hz, 6H, Pt—Me_{eq}), 2.24 (s, 12H, Ar—*Me*), 7.1 (m, 6H, Ar—*H*), 8.75 (s, ^3J(^{195}Pt—H) = 29.7 Hz, 2H, NC*H*).

2.3. Synthesis of [Ar—N=CH—CH=N—Ar]$PtMe_2$ [Ar = 2,6-$Me_2C_6H_3$] (**2**)

The following is an adaption of a published procedure [12]. The diimine ligand (203 mg, 0.77 mmol) was added to a solution of $Pt_2Me_4(\mu\text{-}SMe_2)_2$ (200 mg, 0.35 mmol) in toluene (10 mL). The reaction mixture was stirred for 3 h and filtered, and the solvent was removed under vacuum. The residue was dissolved in ether and filtered before the addition of pentane. Large crystals of the wanted compound formed (85 mg, 54%) after storage at −30 °C for 15 h. ^{1}H NMR (200 MHz, $CDCl_3$) δ 1.66 (s, ^2J(^{195}Pt—H) = 87.6 Hz, 6H, Pt—*Me*), 2.25 (s, 12H, Ar—*Me*), ~7.2 (m, 6H, Ar—*H*), 9.39 (s, ^3J(^{195}Pt—H) = 34.7 Hz, 2H, NC*H*). ^{13}C{^{1}H} NMR (300 MHz, CD_3CN) δ −14.4 (^1J(^{195}Pt—C) = 802.9 Hz, Pt–*Me*), 17.5 (Ar—*C*), 127.3, 128.5, 130.3, 149.2 (^2J(^{195}Pt—C) = 16.0 Hz, C_{ipso}), 165.8 (^2J(^{195}Pt—C) = 10.2 Hz, N=*C*H). Anal. Calc. for $C_{20}H_{26}N_2Pt$: C, 49.07; H, 5.35; N, 5.72; Pt, 39.85. Found: C, 50.03; H, 5.47; N, 5.62; Pt, 38.9%.

2.4. Synthesis of [Ar—N=CH—CH=N—Ar]-$PtMe_3(NCMe)^+OTf^-$ (Ar = 2,6-$Me_2C_6H_3$) (**3** · OTf^-)

A solution of **2** (20.5 mg, 0.042 mmol) in acetonitrile (3 mL) was cooled at −12 °C under an N_2 atmosphere. To this solution, CF_3SO_3Me (5.5 μL, 0.05 mmol, ca. 1 equiv.) was added. The reaction mixture was stirred for

3.5 h during which it was allowed to reach ambient temperature. The color of the mixture changed from deep purple to clear orange. Filtration, evaporation of the solvent, and washing twice with ether left the product as a yellow solid (23.3 mg, 80%). ^{1}H NMR (200 MHz, CD_3CN) δ 0.83 (s, $^2J(^{195}Pt{-}H) = 69$ Hz, 6H, Pt—*Me*), 0.83 (s, $^2J(^{195}Pt{-}H) = 76$ Hz, 3H, Pt—*Me*), 2.12 (s, 3H, C*H*$_3$CN), 2.23 (s, 6H, Ar—*Me*), 2.29 (s, 6H, Ar—*Me*), 7.25 (m, 6H, Ar–H), 8.93 (s, $^3J(^{195}Pt{-}H) = 27$ Hz, 2H, NC*H*C*H*N). $^{13}C\{^1H\}$ NMR (300 MHz, CD_3CN) δ −4.13, −2.89 (Pt—*Me*), 19.1, 19.5 (Ar—*Me*), 129.1, 130.1, 130.2, 130.8, 130.9, 145.6, 171.5. Anal. Calc. for $C_{24}H_{32}F_3N_3O_3PtS$: C, 41.50; H, 4.64; N, 6.05; Pt, 28.08. Found: C, 42.12; H, 4.75; N, 6.45; Pt, 27.82%.

2.5. Generation of [Ar—N=CH—CH=N—Ar]-PtMe(NCMe)$^+$OTf$^-$ (Ar = 2,6-Me$_2$C$_6$H$_3$) (**4**·OTf$^-$) in an NMR tube

To an NMR tube equipped with a Teflon needle valve and vent, **2** (10 mg, 0.02 mmol) was added. Acetonitrile-d_3 (700 μL) was then added by vacuum transfer into the tube. To the resulting solution, triflic acid (2.0 μL, 0.022 mmol) was added. The purple color immediately changed to dark yellow. The ^{1}H NMR spectrum demonstrated quantitative conversion to the same compound that appeared as one of the products in the oxidations that were performed in CD_2Cl_2 (see below). ^{1}H NMR (200 MHz, CD_3CN) δ 0.19 (s, CH_4, ca. 70% obsd. yield), 0.68 (s, $^2J(^{195}Pt{-}H) = 76.3$ Hz, 3H, Pt—*Me*), 2.24 (s, 6H, Ar—*Me*), 2.34 (s, 6H, Ar—*Me*), 7.25 (m, 6H, Ar—*H*), 8.87 (s, $^3J(^{195}Pt{-}H) = 113.5$ Hz, 1H, NC*H*C′H′N′), 8.90 (s, $^3J(^{195}Pt{-}H) = 42.9$ Hz, 1H, NCHC′*H*′N′). $^{13}C\{^1H\}$ NMR (300 MHz, CD_3CN) δ −13.1, 17.7 (Ar—*Me*), 17.9, 129.0, 129.1, 129.3, 129.6, 130.1, 131.3, 145.66, 145.73, 167.7, 176.2.

2.6. Chemical oxidation of **1** in acetonitrile-d_3

Inside a drybox, an NMR tube with a screw cap and septum was loaded with **1** (4.3 mg, 0.0083 mmol) and acetonitrile-d_3 (400 μL). In a glass vial with screw cap and septum, $Cp_2Fe^+OTf^-$ (2.6 mg, 0.0078 mmol, slightly less than 1 equiv.) was dissolved in acetonitrile-d_3 (300 μL). This solution was then transferred to the NMR tube by a syringe, while keeping the tube in the dark to avoid photo-induced reactions. The resulting NMR spectra revealed several Pt—*Me* resonances, including small quantities of unreacted **1**, but the main product and the only identifiable platinum compound was **3**, formed in ca. 70% yield.

2.7. Chemical oxidation of 1 in dichloromethane-d_2

Inside a drybox, an NMR tube with a screw cap and septum was loaded with **1** (7.5 mg, 0.015 mmol), and CD_2Cl_2 (350 μL) was added by syringe. In a glass vial with screw cap and septum, $Cp_2Fe^+OTf^-$ (4.4 mg, 0.013 mmol, slightly less than 1 equiv.) was dissolved in CD_2Cl_2 (350 μL). This solution was transferred to the NMR tube by a syringe, while keeping the tube in the dark to avoid photo-induced reactions. A ^{1}H NMR spectrum was recorded and CH_3CN (50 μL) was added. The resulting NMR spectra displayed mainly **3** and **4** and small quantities of unreacted **1**.

2.8. Constant-potential electrochemical oxidation of 1 in acetonitrile

All electrolysis experiments were performed in an H-shaped cell, the compartments of which were separated by a medium-frit glass junction. Platinum-gauze working electrodes were used. In the experiments, **1** (5.2 mg, 0.01 mmol) was added to acetonitrile/0.05 M $Me_4N^+BF_4^-$ (25 mL) electrolyte in the electrolysis cell. The solutions were electrolyzed at constant potentials until the current had dropped to less than 0.2 mA. The electrolyzed solution was immediately transferred to a round-bottomed flask, and the solvent was removed by vacuum transfer. The residue was extracted with dichloromethane (leaving the electrolyte behind), and the extract was filtered. The dichloromethane was removed from the filtrate. The residue was dissolved in dichloromethane-d_2, and a ^{1}H NMR spectrum was acquired. The electrolyses were performed at $E = 0.7$ V vs. $Cp_2Fe^{0/+}$, and three separate experiments demonstrated the passage of 1.03, 1.01, and 1.00 faraday/mol of charge. The ^{1}H NMR spectrum showed **3** as the only recognizable product. ^{1}H NMR of **3** (200 MHz, CD_2Cl_2): δ 0.86 (s, $^2J(^{195}Pt{-}H) = 71.1$ Hz, 9H Pt–*Me*), ~2.3 (s, 12H, Ar—*Me*), 7.22 (m, 6H, Ar—*H*), 8.99 (s, $^3J(^{195}Pt{-}H) = 26.5$ Hz, 2H, NC*H*).

2.9. Variable-temperature NMR spectra of **3**

^{1}H NMR spectra of **3**·**OTf**$^-$ (~5 mg) in $CDCl_3$ (0.7 mL) were recorded at temperatures ranging from −45 to +55 °C. The spectra were recorded on the Bruker Avance 300 MHz instrument, with evaporation of liquid nitrogen as the cooling source. A small amount (10 μL) of acetonitrile was used to "spike" the sample after the measurements to confirm and identify the resonance corresponding to free acetonitrile. The spectra are further described in the following section.

3. Results and discussion

3.1. Preparative work

The Pt(IV) complex [Ar—N=CH—CH=N—Ar]PtMe$_4$ (**1**) was readily prepared from the diimine ligand and $Pt_2Me_8(SMe_2)_2$ as described in Section 2. The Pt(II) analogue [Ar—N=CH—CH=N—Ar]PtMe$_2$ (**2**) was similarly prepared from the diimine and $Pt_2Me_4(SMe_2)_2$. Treatment of **2** with methyl triflate in acetonitrile generated [Ar—N=CH—CH=N—Ar]PtMe$_3$(NCMe)$^+$OTf$^-$ (**3**·OTf), whereas protonation of **2** in acetonitrile furnished

[Ar—N=CH—CH=N—Ar]PtMe(NCMe)$^{+}$OTf^{-} (**4** · OTf). Species **3** and **4** are of relevance as products from the oxidation of **1** (*vide infra*). The ^{1}H NMR spectra of **1**, **2**, and **4** are quite straightforwardly interpreted, with diagnostic $^{2}J(^{195}\text{Pt—H})$ satellites around the Pt—*Me* resonances, and are consistent with the structures and coordination geometries depicted in Scheme 3.

Whereas the NMR spectra of **1**, **2**, and **4** were straightforwardly assigned and reflected the molecular symmetry, the appearance of the ^{1}H NMR Pt—*Me* signals from **3** were more complicated as they turned out to be highly solvent (Fig. 1) and temperature dependent. The signal arising from the three Pt—*Me* groups appeared as one broadened signal with broadened ^{195}Pt satellites in dichloromethane-d_2 and chloroform-*d*. This indicates that the axial Pt—*Me* group and the two equatorial ones undergo fairly rapid exchange on the measurement time scale. This was corroborated by variable-temperature NMR spectra in $CDCl_3$: at +55 °C, one sharp Pt—*Me* signal is seen as a weighted average for all three methyl groups. Below 0 °C, the axial and at the two equatorial Pt—*Me* groups give rise to separate signals in a 1:2 ratio. It is also noteworthy that at the low-temperature limit, the aryl-*Me* groups of **3** gave rise to two signals that correspond to orientations "above" and "below" the coordination plane of Pt (a consequence of the aryl groups being more or less perpendicularly oriented with respect to the coordination plane, with a sterically imposed restricted rotation around the N—C(aryl) bonds). At the high-temperature limit, these two signals had also undergone coalescence. However, when the spectrum was acquired in acetonitrile-d_3, sharp Pt—*Me* peaks were observed (Fig. 1, bottom). The central peaks of the axial and equatorial Pt—Me groups were however indistinguishable due to coincidental chemical shift equivalence. However, the $^{2}J(^{195}\text{Pt—H})$ couplings for the axial and equatorial Pt—*Me* signals are quite different and two sets of satellites are observed. The fact that the two sets of satellites have not coalesced establishes that rapid interconversion of axial and equatorial methyls does not occur on the measurement time scale in acetonitrile-d_3. Similar dynamic behavior, temperature, and/or solvent effects have previously been observed for other (N—N)PtMe$_3^{+}$OTf^{-} [19–21] complexes. In the present case, this behavior may be understood with Scheme 4 as the basis: In dichloromethane or chloroform solvents, acetonitrile dissociation leads to the five-coordinate intermediate in a medium that contains very little free acetonitrile. The five-coordinate therefore has ample time to scramble the axial and equatorial Pt—*Me* groups before acetonitrile reassociation. On the other hand, in acetonitrile solvent, ligand reassociation occurs much faster, and this inhibits the scrambling process. (Recent isolated five-coordinate Pt(IV) trialkyl species have a near square pyramidal structure with distinct axial and equatorial positions in the solid state; these sites undergo rapid exchange in solution [22–25]). The involvement of acetonitrile dissociation was demonstrated by the addition of 10 μL of acetonitrile to a sample of **3** · OTf in chloroform-*d*. A new resonance arising from the uncoordinated acetonitrile (δ 2.06 at −45 °C) appeared. When the sample was heated to 55 °C, the two resonances from free and coordinated (δ 2.37 at −45 °C) acetonitrile coalesced into one broad peak at δ 2.21, indicating facile exchange between coordinated and uncoordinated acetonitrile at 55 °C.

3.2. Cyclic voltammetry

Acetonitrile/0.1 M $Bu_4N^{+}PF_6^{-}$ and THF/0.2 M $Bu_4N^{+}PF_6^{-}$ solutions of **1** were examined by cyclic voltammetry at 20 °C. In a cyclic voltammogram of the acetoni-

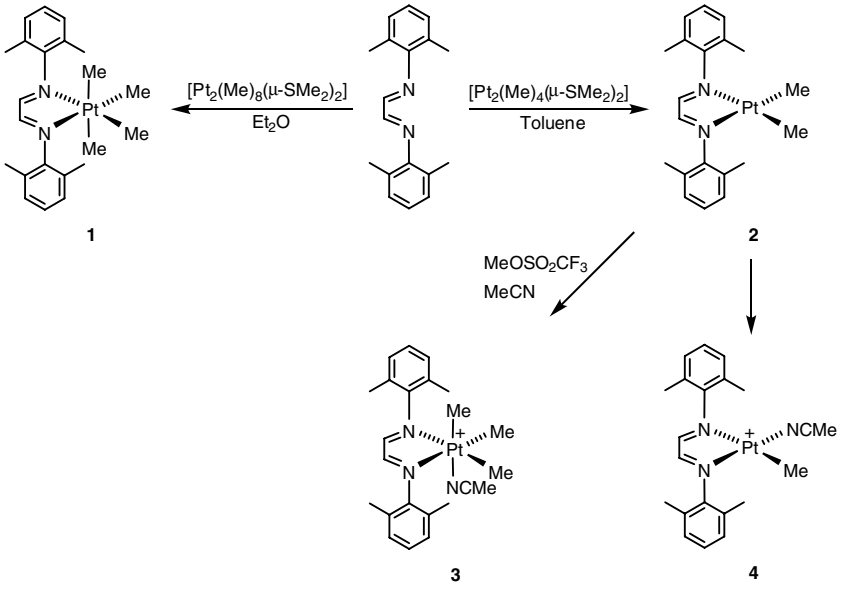

Scheme 3.

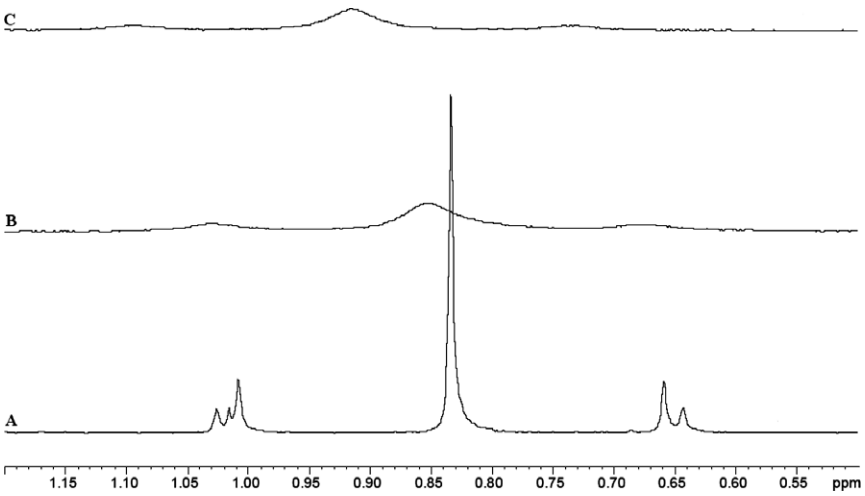

Fig. 1. Pt—*Me* region of the ambient-temperature ^{1}H NMR spectrum of **3** · OTf in three solvents. A: CD_3CN, B: $CDCl_3$, C: CD_2Cl_2.

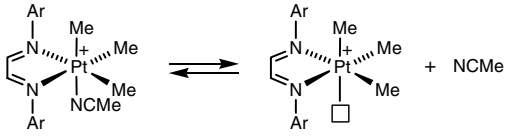

Scheme 4.

trile solution of **1** (Fig. 2, top), two waves can be seen. At −1.47 V vs. $Cp_2Fe^{0/+}$, a reversible reduction produces $\mathbf{1}^{\cdot-}$ via a ligand-based reduction [14] of the diimine moiety. In addition, a chemically irreversible oxidation wave is seen with a peak potential of ca. 0.55 V during the anodic-going scan. These observations qualitatively resemble results previously obtained for **2**, which underwent a ligand-centered reduction at −1.36 V and an irreversible oxidation process at 0.6–0.7 V vs. $Cp_2Fe^{0/+}$ [12]. In THF, the cyclic voltammogram of **1** exhibited two reversible reduction waves at −1.57 and −2.66 V vs. $Cp_2Fe^{0/+}$ respectively and an irreversible oxidation wave at ca. 0.50 V. When the cyclic voltammetry was performed in the opposite direction (anodic sweep first) in acetonitrile, a new reversible wave appeared at −0.96 V, with a peak current ca. 50% of that for the initial oxidation of **1**. This redox couple appears to arise from a product that must be formed by reaction of $\mathbf{1}^{\cdot+}$ that was generated as a transient during the irreversible oxidation. This reversible wave is attributed to the cationic Pt(IV) species **3**, which was voltammetrically observed and isolated after an exhaustive electrolysis of **1** in acetonitrile (*vide infra*). The assignment of this oxidation wave is further supported by an earlier report on closely related complexes [12]. The presence of **3** is readily seen as a persistent wave in Fig. 1, bottom, which depicts a multi-scan cyclic voltammogram in which each scan is immediately followed by a new one. (The apparent reversibility of the oxidation wave at +0.5 V in this voltammogram is an artifact caused by fouling of the electrode surface.)

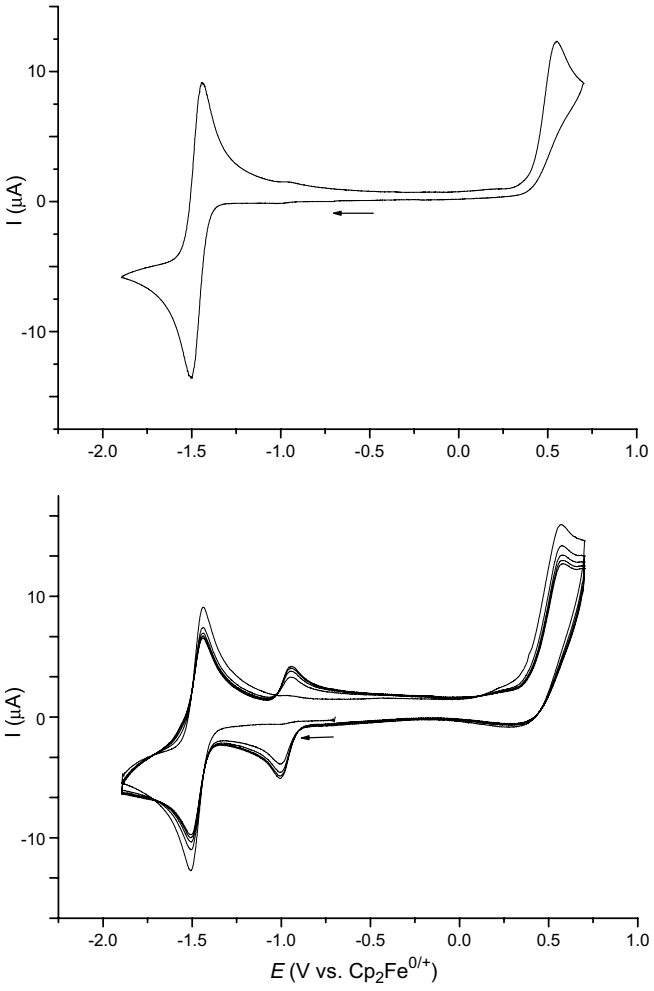

Fig. 2. Cyclic voltammograms for **1** with an initial cathodic-going scan direction. Conditions: 1 mM solution in acetonitrile/0.1 M $Bu_4N^+PF_6^-$ at 20 °C ($d = 0.6$ mm Pt disc electrode, voltage sweep rate $v = 1$ V/s). Top: Single-scan CV. Bottom: Continuous multi-scan CV.

3.3. Exhaustive electrolysis of *1*

To elucidate the nature of the product that was observed by cyclic voltammetry after the irreversible oxidation of **1**, exhaustive electrochemical bulk oxidation was performed. An acetonitrile/0.05 M $Me_4N^+BF_4^-$ solution of **1** was oxidized at a Pt mesh electrode at a working electrode potential of +0.7 V vs. $Cp_2Fe^{0/+}$. Three separate experiments demonstrated the passage of 1.0 faraday/mol of charge, i.e. the oxidation of **1** is a one-electron process. The solution from the anodic compartment of the electrolysis cell was collected, the solvent was evaporated, the solid residue extracted with dichloromethane (leaving the electrolyte behind) and filtered, and the solid material was investigated by ^{1}H NMR spectroscopy. The ^{1}H NMR spectrum demonstrated that [Ar—N=CH—CH=N—Ar]$PtMe_3$-$(NCMe)^+$ (**3**) was the major product, and in fact the only recognizable product of the electrochemical oxidation. This discounts the possible formation of **4** under these conditions.

3.4. Chemical oxidation of *1*

Ferrocenium triflate $Cp_2Fe^+OTf^-$ was selected as a homogeneous oxidant despite the fact that the electron-transfer from **1** to Cp_2Fe^+ is strongly unfavorable based on the observed irreversible peak oxidation potential for **1**: The unfavorable electron-transfer should eventually be driven to completion by the rapid follow-up reaction that consumes $\mathbf{1}^{\cdot+}$. (A similar approach was used when the oxidation of analogues of **2** was investigated [12]). Indeed, when $Cp_2Fe^+OTf^-$ was added to a solution of **1** in acetonitrile-d_3 in a sealed NMR, a slow change in color from dark purple to brown was observed. The reaction resulted in a complex reaction mixture with a number of ^{1}H NMR signals that could be attributed to Pt—*Me* protons. An analysis of the ^{1}H NMR spectrum from the oxidation of **1** revealed that **3**-d_3 (containing a deuterated acetonitrile ligand) was the major (ca. 70% yield) Pt—*Me* containing product, and also the only identifiable Pt—*Me* containing product. Importantly, there were no detectable quantities of the Pt(II) cation **4** among the minor products. Methane or ethane, which might result from oxidatively induced Pt—Me homolysis or concerted reductive eliminations, respectively, were not detected by ^{1}H NMR when the chemical oxidation was performed in acetonitrile-d_3. Concerning the fate of the fourth methyl group in **1**, which must somehow be cleaved off when **3** is formed, it is important to note that methylferrocene, $(C_5H_4Me)(C_5H_5)Fe$, is formed in addition to ferrocene itself. The α and β protons of the substituted Cp ring appear as an AA′BB′ pattern at δ 3.92–4.08, readily distinguished from the overlapping signals of the Cp rings of ferrocene and methylferrocene at δ 4.13. Integration of the α and β proton signals indicated a ca. 3:1 molar ratio of ferrocene to methylferrocene. The overall stoichiometry of the reaction appeared to be 1:1 Cp_2Fe^+ to Pt in acetonitrile, in agreement with the exhaustive electrolysis experiments described above. The findings are qualitatively summarized (but not stoichiometrically balanced) in Scheme 5, top.

When dichloromethane-d_2 was used for a similar oxidation reaction, resonances that might result from [Ar—N=CH—CH=N—Ar]$PtMe_3(L)^+$ and [Ar—N=CH—CH=N—Ar]$PtMe(L)^+$ (L = OTf^- or CD_2Cl_2) species were seen in a rather complex spectrum with numerous overlapping signals (the combined yield is impossible to accurately measure but is estimated at ca. 50–60%). These species differ from **3** and **4** only in the identity of the auxiliary ligand L. These assignments are supported by the finding that addition of acetonitrile to the solution after complete oxidation produced **3** and **4**, readily identified by NMR (see above). The oxidation in dichloromethane-d_2 also led to the production of substantial quantities of ethane, qualitatively identified by ^{1}H NMR and by mass spectrometry analysis of the headspace above the solution after opening of the NMR tube. The stoichiometry of the reaction appeared to be ca. 1:1 Cp_2Fe^+ to Pt also in dichloromethane; again, the ferrocene was accompanied by methylferrocene, but the latter was seen in smaller quantities than was the case in acetonitrile. The findings are summarized (but not stoichiometrically balanced) in Scheme 5, bottom.

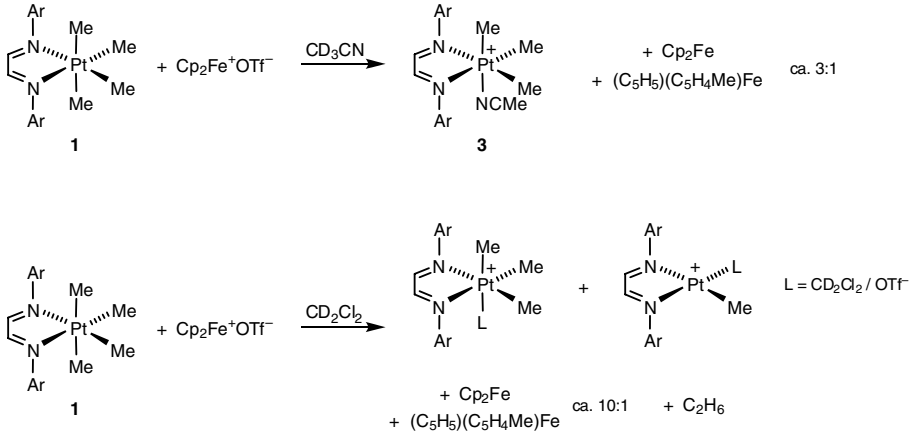

Scheme 5.

Unfortunately, we have not succeeded with completely accounting for the mass balance in these reactions, and this will necessarily render any mechanistic discussion very uncertain. However, some main features and inferences will be presented in the following.

3.5. Mechanistic implications

In agreement with observations made on a related system by Kaim and co-workers [14], we find that the Pt(IV) complex [Ar—N=CH—CH=N—Ar]$PtMe_4$ is at least as readily oxidized as the Pt(II) analogue [Ar—N=CH—CH=N—Ar]$PtMe_4$, as inferred from the irreversible cyclic voltammetry oxidation waves. As expressed by Kaim, the strong donor methyl groups therefore offset the effect of the higher formal oxidation state of Pt. The previous study [14], which was supported by DFT calculations and electronic spectra, showed that the HOMO of the Pt(IV) species is an antisymmetric Pt—C_{axial} σ-orbital combination mixed with some p_π (Pt) contributions. A one-electron oxidation of **1** therefore should tend to weaken the axial Pt—*Me* bonds and the incipient cation $\mathbf{1}^{\cdot+}$ should be activated with respect to Pt—C bond cleavage, be it by homolytic Pt—C cleavage or concerted C-C bond coupling reactions.

An oxidatively induced reductive elimination of ethane from $\mathbf{1}^{\cdot+}$ would produce $\mathbf{2}^{\cdot+}$ in addition to ethane, and the Pt-containing products should then be the same as those seen during the oxidation of **2** and analogues, i.e. a 1:1 mixture of **3** and **4** resulting from intermolecular methyl group transfer. Since oxidation of **1** in acetonitrile does not produce ethane, results in only **3** and *not* **4**, and oxidation with Cp_2Fe^+ produces significant amounts of methylferrocene (which was not observed when Pt(II) species were oxidized [12]), it is apparent that the initial reaction cannot be a simple reductive elimination. Instead, we propose that the incipient $\mathbf{1}^{\cdot+}$ with its weakened axial Pt—*Me* bonds undergoes homolytic cleavage of a Pt—C bond. This leaves the five-coordinate fragment [Ar—N=CH–CH=N—*Ar*]$PtMe_3^+$ which, in acetonitrile solution, is efficiently trapped to produce **3** as the only observable Pt product. The fate of the lost methyl group is, unfortunately, to a great extent unknown. The appearance of methylferrocene does however suggest that at least in part, Cp_2Fe^+ is capable of acting as a methyl radical acceptor; methyl transfer to one Cp ring in Cp_2Fe^+ produces protonated methylferrocene as the obvious precursor to methylferrocene. Thus far, the resulting stoichiometry would be 2:1 Cp_2Fe^+ to Pt contrasting the observed 1:1 stoichiometry. The accompanying proton that would be generated might be a source of methane by protonation of Pt—*Me* containing species; however, methane was never observed. Alternatively, the proton might act as a one-electron oxidant towards **1** or Cp_2Fe; in this case, a 1:1 stoichiometry would result in accordance with observations.

The oxidation of **1** with Cp_2Fe^+ in dichloromethane-d_2 produced different products from those seen in acetonitrile-d_3. In dichloromethane-d_2, ethane is observed, along with the formation of **3** *and* **4**. We surmise that Pt—C homolytic cleavage still occurs (evidenced by the appearance of methylferrocene). However, there is now a possibility that direct ethane elimination occurs from $\mathbf{1}^{\cdot+}$; the resulting $\mathbf{2}^{\cdot+}$ would then give rise to **3** and **4** by a mechanism analogous to that described earlier [12] for the oxidation of (diimine)$PtMe_2$ complexes.

3.6. Concluding remarks

In this study, we have demonstrated that closely related Pt(IV) and Pt(II) species undergo facile oxidation reactions under quite similar reaction conditions to give similar – but not completely identical – products and product distributions. These findings suggest that when redox processes are involved in catalytic cycles that involve Pt(II) and Pt(IV) species, it may be useful to keep in mind that oxidation of Pt(IV) species should also be considered as a key to understanding the overall process and the resulting product distributions.

Acknowledgements

We gratefully acknowledge financial support from the Norwegian Research Council (NFR) in the form of a stipend to B.J.W. and generous contributions from the NMR facilities at the Department of Chemistry, University of Oslo.

References

[1] J.L. Garnett, R.J. Hodges, J. Am. Chem. Soc. 89 (1967) 4546.
[2] R.J. Hodges, J.L. Garnett, J. Phys. Chem. 72 (1968) 1673.
[3] A.E. Shilov, G.B. Shul'pin, Chem. Rev. 97 (1997) 2879.
[4] N.F. Gol'dshleger, M.B. Tyabin, A.E. Shilov, A.A. Shteinman, Zh. Fiz. Khim. 43 (1969) 2174.
[5] A.E. Shilov, G.B. Shul'pin, Activation and Catalytic Reactions of Saturated Hydrocarbons in the Presence of Metal Complexes, Kluwer Academic, Dordrecht, 2000.
[6] M. Lersch, M. Tilset, Chem. Rev. 105 (2005) 2471.
[7] U. Fekl, K.I. Goldberg, Adv. Inorg. Chem. 54 (2003) 259.
[8] S.S. Stahl, J.A. Labinger, J.E. Bercaw, Angew. Chem., Int. Ed. 37 (1998) 2181.
[9] H. Heiberg, L. Johansson, O. Gropen, O.B. Ryan, O. Swang, M. Tilset, J. Am. Chem. Soc. 122 (2000) 10831.
[10] L. Johansson, M. Tilset, J.A. Labinger, J.E. Bercaw, J. Am. Chem. Soc. 122 (2000) 10846.
[11] H.A. Zhong, J.A. Labinger, J.E. Bercaw, J. Am. Chem. Soc. 124 (2002) 1378.
[12] L. Johansson, O.B. Ryan, C. Rømming, M. Tilset, Organometallics 17 (1998) 3957.
[13] J.D. Scollard, M. Day, J.A. Labinger, J.E. Bercaw, Helv. Chim. Acta 84 (2001) 3247.
[14] W. Kaim, A. Klein, S. Hasenzahl, H. Stoll, S. Zális, J. Fiedler, Organometallics 17 (1998) 237.
[15] J.M. Kliegman, R.K. Barnes, J. Org. Chem. 35 (1970) 3140.
[16] M. Lashanizadehgan, M. Rashidi, J.E. Hux, R.J. Puddephatt, S.S.M. Ling, J. Organomet. Chem. 269 (1984) 317.
[17] J.D. Scott, R.J. Puddephatt, Organometallics 2 (1983) 1643.

[18] Z.W. Li, A. Yeh, H. Taube, Inorg. Chem. 33 (1994) 2874.
[19] G.S. Hill, G.P.A. Yap, R.J. Puddephatt, Organometallics 18 (1999) 1408.
[20] R.M. Gschwind, S. Schlecht, J. Chem. Soc., Dalton Trans. (1999) 1891.
[21] R. van Asselt, E. Rijnberg, C.J. Elsevier, Organometallics 13 (1994) 706.
[22] U. Fekl, W. Kaminsky, K.I. Goldberg, J. Am. Chem. Soc. 123 (2001) 6423.
[23] S. Reinartz, P.S. White, M. Brookhart, J.L. Templeton, J. Am. Chem. Soc. 123 (2001) 6425.
[24] U. Fekl, K.I. Goldberg, J. Am. Chem. Soc. 124 (2002) 6804.
[25] U. Fekl, W. Kaminsky, K.I. Goldberg, J. Am. Chem. Soc. 125 (2003) 15286.